

Static skin effect and acoustoelectric instability in filamentous bismuth single crystals

Yu. A. Bogod, D. V. Gitsu, and A. D. Grozav

Low-Temperature Physicotechnical Institute, Academy of Sciences of the Ukrainian SSR, and Institute of Applied Physics, Academy of Sciences, Moldavian SSR

(Submitted 1 July 1985)

Zh. Eksp. Teor. Fiz. **90**, 1010–1021 (March 1986)

The I - V characteristics and ohmic magnetoresistance R_H^d of filamentous bismuth single crystals of thickness 1 – $10\ \mu\text{m}$ are studied in a transverse magnetic field $\mathbf{H} \perp \mathbf{C}_2$. For strong magnetic fields and sufficiently low temperatures, the I - V characteristic has a “kink” which enhances the magnetoresistance and is due to longitudinal generation of phonons in the skin layer. The corresponding current density j_k^H drops below the value j_k^0 , $\sim nes$ for $H = 0$ by an amount which is proportional to the Larmor radius r , where s is the speed of sound. Under the experimental conditions, the transition to phonon generation serves as a reliable indication of the current density distribution over the sample, and it is shown that the current density in the bismuth crystals is concentrated in a surface layer of thickness $\sim r$. The ohmic magnetoresistance peaks as a function of temperature, and the maximum occurs at lower temperatures T_m as the crystal thickness increases; however, T_m is independent of the magnetic field strength. The ratio R_H^d/H is a minimum when the extreme orbit diameter $D_{\text{ext}}^{e2,3}$ for the electrons in the equivalent 2.3 ellipsoids is $\approx d$, where d is the crystal thickness. The calculated I - V characteristic describes the onset of acoustoelectric instability when longitudinal generation of phonons occurs. This I - V characteristic and the static skin theory for $r/\tilde{d}l \lesssim 1$ are used to analyze the experimental results and estimate the probability for intervalley scattering of the \tilde{d} electrons by the crystal surface. The electron mean free path l is also estimated.

The static skin effect involves the expulsion of a dc electric current toward the surface of a conductor due to differences in the electron motion in the interior and at the surface. This effect, which has been analyzed theoretically in Refs. 1–6, can be described physically as follows. In compensated conductors (we confine ourselves to a conducting plate in a strong magnetic field which is parallel to the plate surface and perpendicular to the current), the dissipative current is determined by collision-induced displacements of the centers of the Larmor orbits. Inside the crystal the orbit centers are displaced by an amount $\sim r$ during the mean collision time τ , where r is the Larmor radius. If we assume a unit probability for intervalley (electron-hole) scattering at the surface, if the scattering is coherent,⁷ and if the electron and hole orbits have equal radii, then the carriers near the surface also move a distance $\sim r$ during τ , and the conductivity σ_H inside the crystal and near the surface is $\sim \sigma_0(r/l)^2$, where σ_0 is the bulk conductivity in the absence of a magnetic field. If the surface scattering is coherent but the orbit radii differ considerably and electron-hole recombination is either improbable or forbidden altogether by the structure of the surface, then the carriers move a distance $\sim l$ along the surface during the time τ , where the mean free path $l \sim v_F \tau$ is determined by volume scattering processes. If the intra- and inter-valley relaxation times in the interior are comparable ($\tau \sim \tau_r$), then the dc current becomes concentrated in a boundary layer of thickness $\sim r$ and conductivity $\sim \sigma_0$. However, when $\tau \ll \tau_r$ (as in the case for bulky semimetals at low temperatures⁸), the particle concentration distribution in the valleys must change in order for the normal current

across the surface to vanish. The concentration gradient decreases away from the surface at distances comparable to the intervalley diffusion length $L_1 \sim r(\tau_r/\tau)^{1/2}$. An expression for the boundary layer conductivity σ of semimetals was first derived in Ref. 4; σ is equal to σ_0 , the conductivity of a skin layer of thickness r , times the number L_1/r of electron gyrations in the skin layer. In fact, because of diffusion we may replace L_1/r by $r/\tilde{d}l$ (Ref. 5), where \tilde{d} is the intervalley scattering probability at the surface, L_1/r is the number of gyrations in the skin layer when recombination is neglected, and $r/\tilde{d}l$ is the corresponding value corrected for the limiting effects of surface recombination. According to Ref. 5, the conductivity of the diffusion layer increases because the repeated reentry of carriers into the skin layer and their unbounded movement along the surface result in the formation of an extended orbit along which the electrons gain energy in the external field.

It seems plausible that under suitable conditions, the static skin effect might radically alter the I - V characteristics of conductors. This can be illustrated by considering the onset of acoustoelectric instability. For large compensated conductors, for which the skin layer has little influence on the magnetoresistance, phonon generation is detected at current densities $j \sim nes(r/l)$, where n is the carrier concentration and s is the speed of sound. This type of instability is due to ultrasonic drifting of carriers in the plane normal to the current ($v_d^1 \approx cE/H > s$, where E and H are the electric and magnetic field strengths) and is accompanied by a significant increase in the conductivity.^{9–10} We consider a compensated conductor of thickness d with a skin layer $h \ll d$; the

TABLE I.

Specimen	Diameter, 10^{-4} cm	Length, cm	$R_0^{300}/R_0^{4.2}$	$\mu_0^{4.2}, 10^8$ $\text{cm}^2/\text{V} \cdot \text{s}$	$\bar{d}, 10^{-2}$
Bi-1A1	1.0	0.381	14.7	3.17	0.66
Bi-1A2	1.0	0.384	15.6	3.36	0.66
Bi-2B1	2.0	0.330	18.3	3.94	—
Bi-3B14	2.8	0.329	15.1	3.25	0.74
Bi-3B15	3.4	0.429	11.2	2.41	1.10
Bi-3B16	3.4	0.434	17.4	3.75	1.00
Bi-3B17	3.4	0.279	17.6	3.79	—
Bi-3B18	3.4	0.434	20.4	4.39	1.00
Bi-4B4	4.0	0.170	—	—	—
Bi-10B1	10.3	0.323	7.3	1.57	3.00
Bi-10B2	10.3	0.328	8.1	1.75	3.00

skin layer conductivity is assumed to be σ_0 for crossed E and H fields, and $(r/l)^2 \ll h/d$. It is easy to see that in this case, the condition $v_a^1 \sim cE/H = s$ can be satisfied for current densities $j_{k_2}^H \sim nes(l/r)(2h/d)$, whereas in the skin layer, phonon generation along the drift field begins at an average current density $j_{k_2}^H \sim nes(2h/d) \ll j_{k_2}^H$. Longitudinal phonon generation is known to increase the resistance,¹¹⁻¹⁴ and for this reason the I - V characteristics may differ qualitatively for thin and thick conductors when acoustoelectric instability occurs.

Structurally perfect bismuth single crystals are well-suited for experimental verification of the above conclusions. In addition to the small ratio of the surface to the volume magnetoresistance, acoustoelectric instability in these crystals occurs at relatively low electric fields. The experiments described in this paper were carried out using slender Bi single crystals of thickness from 1 to $10 \mu\text{m}$ (we previously studied¹⁴ acoustoelectric instability in such crystals for $H = 0$). The principal results may be summarized as follows.

1. Under certain conditions, the I - V characteristics for bismuth in a strong ($r \ll l, d$) transverse magnetic field have a "kink" which corresponds to the onset of acoustoelectric instability. This kink enhances the magnetoresistance, and the corresponding critical current density $j_{k_1}^H$ drops below the value $j_{k_1}^0 \approx nes$ for $H = 0$ by an amount which is proportional to the Larmor radius. The extreme diameter $D_{\text{ext}}(H)$ of the electron orbit calculated from the relation $j_{k_1}^H \approx j_{k_1}^0 D_{\text{ext}}(H)/d$ is in reasonable agreement with the characteristic dimension of the Fermi surface for bismuth under the experimental conditions.

2. The ohmic magnetoresistance of the slender Bi crystals peaks at a temperature T_m which decreases as the crystal thickness d increases. However, T_m is independent of H .

We regard our results as constituting a direct experimental proof that when a transverse magnetic field is applied to current-carrying conductors, the current may become concentrated within a surface layer of width $h \sim r$. The kink in the I - V characteristic is associated with longitudinal generation of phonons in the skin layer, where the static skin-effect theory for the case $L_1 \gg r^2/\bar{d}l$ describes the experimental data on the linear part of the characteristic. In this model, the temperature peak in the magnetoresistance is deter-

mined by the condition that the surface and bulk conductivities be equal.

EXPERIMENTAL RESULTS

We studied cylindrical crystals insulated by Pyrex glass; the long axis of the crystals made a 19.5° angle with the C_1 axis in the bisecting C_1C_3 trigonal plane. The crystals were prepared and mounted as described in Refs. 14-16, and their properties are summarized in Table I. The ohmic magnetoresistance was measured under steady-state conditions for $4.2 \leq T \leq 77$ K. The crystal and heater were inserted into an ampul filled with heat-exchanging gas to a pressure of 10^{-2} - 10^{-3} torr. The I - V characteristics were recorded under both steady-state and pulsed conditions. In the former case the current was specified exactly, while in the latter case

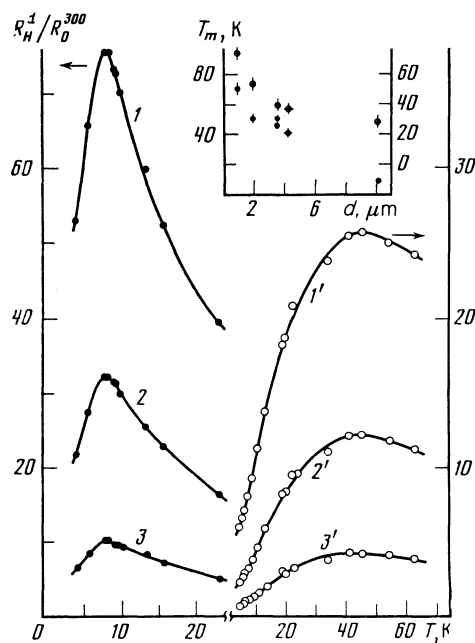


FIG. 1. Ohmic magnetoresistance as a function of temperature. The insert shows the temperature T_m at which R_H^4/R_0^{300} is a maximum for several crystal thicknesses (the left- and right-hand vertical axes correspond to $\mathbf{H} \perp C_2$ and $\mathbf{H} \parallel C_2$, respectively). Curves 1, 2, 3, and 1', 2', 3' are for specimens Bi-10V1 and Bi-3V18 in magnetic fields $H = 17.1, 10.4,$ and 5.3 kOe.

TABLE II.

H, kOe	Bi-10V1			Bi-3B18		
	T, K					
	4.3	8.2	23.2	4.6	45.5	62.9
5.3	47.3	52.6	13.7	13.1	13.8	10.3
10.4	158.2	167.3	46.9	44.9	41.8	32.3
17.1	385.0	393.0	113.4	117.9	90.0	71.0

the desired currents were closely approximated. The G5-27A generator produced square-wave current pulses of length 1–10 μ s, and the crystals were immersed directly into the liquid helium while the I - V characteristics were recorded. Except for the insert in Fig. 1, all the values reported below were obtained for $\mathbf{H} \perp C_2$.

Figure 1 shows the temperature dependence $R_H^d(T)$ of the ohmic magnetoresistance for Bi-3V18 and Bi-10V1 crystals. The insert shows the characteristic peak, whose location T_m depends on the crystal thickness. For $d \leq 4 \mu\text{m}$, T_m is independent of the magnetic field vector \mathbf{H} to within the measurement error. However, for $d = 10.3 \mu\text{m}$ and $\mathbf{H} \perp C_2$, T_m is lower than for the case when $\mathbf{H} \parallel C_2$. T_m is virtually independent of the magnetic field strength. Finally, for $4.2 \leq T < T_m$ the specific magnetoresistance behaves as $\rho_H^d(T) - \rho_H^d(4.2 \text{ K}) \propto T^2$.

Table II lists the relative magnitudes of the magnetoresistive effect

$$\Delta R_H^d / R_0^d = [R_H^d(T) - R_0^d(T)] / R_0^d(T)$$

at several points on the curves $R_H^d(T) / R_0^{300}$, where R_0^d is the electric resistance at zero magnetic field for a crystal of thickness d and R_0^{300} is the corresponding value at $T = 300 \text{ K}$. For $1 \leq d \leq 10 \mu\text{m}$, the specific resistance ρ_0^{300} at room temperature is the same as for bulk crystals.¹⁷ A transition from increasing to decreasing $\Delta \rho_H^d(T)$ was noted in Ref. 18 for a plate consisting of antimony "whiskers" when a magnetic

field parallel to the plate surface was present [no information regarding the dependences $T_m(d)$ and $T_m(H)$ was given in Ref. 18].

A rise in R_H^d was reported in Ref. 6 for bismuth plates for thickness $\approx 1 \text{ mm}$ in the interval $1.4 \leq T \leq 4.2 \text{ K}$ when a magnetic field 200–300 Oe was aligned parallel to the surface (no measurements were carried out for $T > 4.2 \text{ K}$). This finding was attributed⁶ to a linear term $\rho_1 H$ in the magnetoresistance; however, the nature of this term was not determined. According to our data, for fields $2 \leq H \leq 20 \text{ Oe}$ and $T = \text{const}$, $\Delta \rho_H^d(H)$ in all cases obeys a single dependence of the type $\rho_2 H^N$, where the exponent N is slightly less than 2. We found that even if the linear term $\rho_1 H$ is actually present,¹⁾ the relation $\rho_1 H \sim \rho_2 H^N$ can hold only for magnetic fields below 1 kOe. Thus in any event, for fields $H \approx 10 \text{ kOe}$ the linear term in the magnetoresistance can contribute at most 10%, and the dominant contribution to $\Delta \rho_H^d(T)$ comes from $\rho_2 H^N$. For our crystals, the relation $\rho_0^d \sim \rho_H^d$ holds for strong magnetic fields (Fig. 2).

Figure 3 shows the initial portions of the I - V characteristics for a Bi-3V16 crystal in a transverse magnetic field at $T = 4.2 \text{ K}$. The arrows indicate the currents $j_{k_1}^H$ and fields $E_{k_1}^H$, above which Ohm's law starts to break down.²⁾ For large H , we find $j_{k_1}^H \propto H^{-1}$ and $E_{k_1}^H \propto H$ to within the experimental error. For crystals of thickness $d = 10.3 \mu\text{m}$, the dependence $j_{k_1}^H \propto H^{-1}$ persisted for all H considered in the experiments (Figs. 4,5). For $H = 0$, $j_{k_1}^0$ was $\approx 4.8 \cdot 10^3 \text{ A/cm}^2$ for all of the crystals.

Figure 6 shows some I - V characteristics for specimen Bi-3V17 in a wide range of electric fields. We see that for

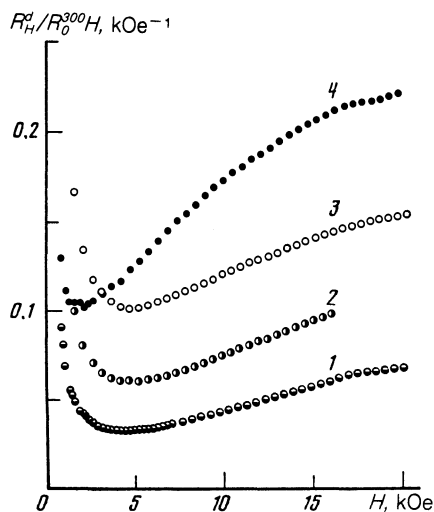


FIG. 2.

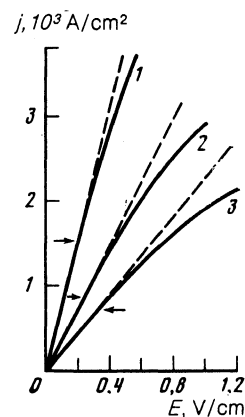


FIG. 3.

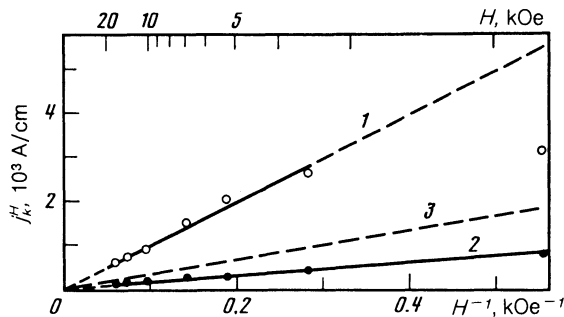


FIG. 4.

fields $E_{k_2}^H$ satisfying $cE_{k_2}^H/H \gtrsim s$, the I - V curve contains a second breakpoint which is reminiscent of the familiar Esaki effect in bulky bismuth single crystals.^{9,10} The acoustic emf $E_a(j/j_k^H)$ decreases with increasing H and T between the first and second kinks.

To estimate the heating at the breakpoints, we note that near the first kink, the power Φ_s^i calculated per unit surface area of the Pyrex capillary is $\approx 0.25 \cdot 10^{-2} \text{ W/cm}^2$ for specimen Bi-3V16; this is less than one percent of the threshold power $q_c^{4.2}$ for the transition from bubble to film boiling in liquid helium. The heating ΔT of the crystal relative to the thermostat was therefore less than 10^{-2} K ($\Delta T \sim \Phi \ln(D/d)/2\pi L\lambda$, where Φ is the evolved power, D and L are the external diameter and length of the insulating Pyrex capillary, and λ is the thermal conductivity of the Pyrex). The critical heat transfer is apparently responsible for the jump in the field with increasing current; indeed, this jump occurs precisely when $\Phi_s^i \approx q_c^{4.2} \approx 0.5$ – 0.7 W/cm^2 . The specific electric power evolved in the crystal can be found from the formula $\Phi_v = j(E - E_a)$ (Ref. 14), where the acoustic emf E_a is determined as shown in the insert to Fig. 6. The I - V characteristics for specimen Bi-3V17 were recorded for $H = 3.5, 7,$ and 13.6 kOe and contain jumps at $j \approx 4 \cdot 10^4, 2.25 \cdot 10^4,$ and $1.23 \cdot 10^4 \text{ A/cm}^2$ ($\Phi_s^i \approx 0.7 \text{ W/cm}^2$). Under these conditions the crystal was $\sim 1 \text{ K}$ warmer than the outer surface of the Pyrex capillary. The steady-state and pulsed I - V characteristics (curves and points in Fig. 6, respectively) coincide for $\Phi_s^i < 0.7 \text{ W/cm}^2$.

Near the second kink on the I - V curve for specimen Bi-3V17 (Fig. 6, pulsed fields) we have $\Phi_s^i \approx 2$ and 5 W/cm^2 for $T = 4.2$ and 20.4 K , respectively. Before the heating can be estimated at these powers, we must know whether heating

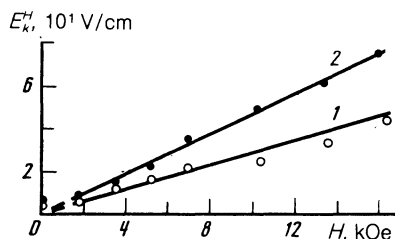


FIG. 5.

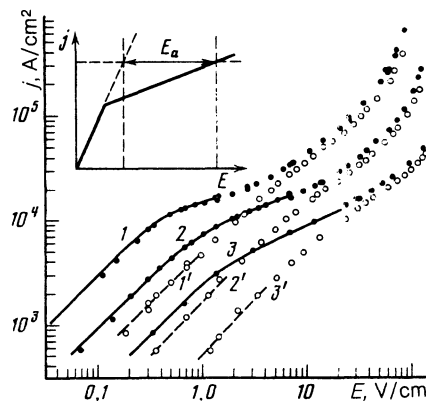


FIG. 6.

occurs ballistically or by diffusion, as well as the amount of heat that is actually transferred to the liquid helium for pulses of length 1 – $10 \mu\text{s}$ ($q_c^{20.4} \approx 11.3 \text{ W/cm}^2$ according to Ref. 19).

What little information is available¹⁹ suggests that times $t \gtrsim 10^{-3} \text{ s}$ are required for significant transient heating to occur in liquid helium when $\Phi_s^i \approx 2 \text{ W/cm}^2$. Furthermore, the thermal conductivity data in Ref. 20 indicate that the phonon mean free path l_{ph} is only $\approx 10^{-3} \text{ cm}$ in dielectric glasses at $T \approx 4.2 \text{ K}$ —i.e., l_{ph} is comparable to the thickness $l_i \approx 1.2 \cdot 10^{-3} \text{ cm}$ of the capillary wall. On the other hand, l_{ph} is known to increase significantly for acoustic powers above 10^{-7} W/cm^2 ; indeed, because of the “acoustic transparency” effect in glasses,²⁰ l_{ph} is ~ 1 – 10 cm for $\Phi_s^i \sim 10^{-4} \text{ W/cm}^2$. If heating occurred by the ballistic mechanism, the Bi-3V17 specimen would be only a few tenths of a degree warmer than the liquid helium thermostat for currents and fields $\approx j_k^H, E_{k_2}^H$. (The formula used to calculate the heating in the ballistic case was taken from Refs. 21–23, as well as data on the phonon transmission coefficients for the metal/glass and solid/liquid helium interfaces.) For the diffusion-dominated case, the crystal should heat up by $\Delta T \sim 10 \text{ K}$ for both $T = 4.2$ and $T = 20.4 \text{ K}$; one thus cannot rule out the possibility that heating might be responsible for the second breakpoint on the I - V characteristic. We estimated ΔT for the case $l_{ph} \lesssim l_i$ by the following method. First we calculated the thermal relaxation time t_T from the relation $\lambda t_T / \rho C a^2 \sim 1$ – 10 (Ref. 24), where $\rho, C,$ and λ are the density, specific heat, and thermal conductivity of the Pyrex, and $a \sim d$. For $T = 20.4 \text{ K}$, t_T is comparable to the length 10^{-5} – 10^{-6} s of the current pulse, while at 4.2 K t_T is $\sim 10^{-7} \text{ s}$. These values are somewhat too low, because we have assumed that C and λ are independent of temperature. Thus, under our experimental conditions we may use the above formula for a steady-state heat flux across the capillary surface to estimate the heating ΔT .

DISCUSSION

1. We will assume that when $E \gg E_{k_1}^H$, phonons are generated along the direction of the current in a surface layer of

width h in the conductor. Then if $h \ll d$ and the surface conductivity is much greater than the bulk conductivity, h can be found from the relation $j_{k_1}^H \approx j_{k_1} (2h/d)$. Here $j_{k_1}^H = 4I_{k_1}^H/\pi d^2$ is the average current density in the crystal at the kink on the I - V characteristic, and j_{k_1} is the current density in the conducting layer due to carriers that drift longitudinally at the speed of sound s . We can in turn find j_{k_1} by measuring the I - V characteristic at zero magnetic field. This procedure for determining the depth of the conducting layer is justified only if the relative contributions to the electron (e) and hole (p) currents from the different valleys are the same for $H \neq 0$ and for $H = 0$. A calculation shows that for $\mathbf{j} \parallel C_1$ and $\mathbf{H} \perp C_2$ in bismuth, electrons from the equivalent "2.3 ellipsoids" completely determine both σ_H and σ_0 to within 10%. If we set $j_{k_1} \approx j_{k_1}^0$ ($j_{k_1}^0 \approx 4.8 \cdot 10^3$ A/cm², cf. above) under our conditions, and $\mathbf{H} \perp C_2$, $H \sim 10$ kOe, we obtain $2h \approx 3.7 \cdot 10^{-5}$ and $6.2 \cdot 10^{-5}$ cm for the Bi-10V2 and Bi-3V16 specimens, respectively.³⁾ On the other hand, according to Ref. 27 the extremal diameter $D_{\text{ext},3}^{e,2.3}$ of the electron orbit in the C_2 direction lies between $3.75 \cdot 10^{-5}$ and $4.7 \cdot 10^{-5}$ cm for our experimental geometry (here and below, we consider the dimensions of orbits in a 10 kOe field). The larger value is obtained by extrapolating the angular dependence of the Fermi momenta p_F using the ellipsoidal model, while the second smaller figure corresponds to the experimental points in Ref. 27.⁴⁾

The fact that the electrons in the 2.3 ellipsoids give the decisive contribution to the measured magnetoresistance provides independent confirmation of the results shown in Fig. 2. Since R_H^d behaves differently in magnetic fields for $D_{\text{ext}} < d$ and for $D_{\text{ext}} > d$, the minimum on curves 3 and 4 must be taken to correspond precisely to the condition $D_{\text{ext}} \approx d$. This implies that $D_{\text{ext}} \approx (4-4.5) \cdot 10^{-5}$ cm $\approx D_{\text{ext},3}^{e,2.3} \approx 2h$.

If the current is concentrated at a distance $h \approx D_{\text{ext},3}^{e,2.3}/2$ from the surface, then the proportionality $j_{k_1}^H \propto r \propto H^{-1}$ valid for $D_{\text{ext}} \ll d$ should break down for fields $H \approx 1-2$ kOe in a crystal of thickness $3.4 \mu\text{m}$. For a $10.3\text{-}\mu\text{m}$ -thick crystal, $D_{\text{ext},3}^{e,2.3} < d$ continues to hold for these fields, and the $j_{k_1}^H (H^{-1})$ dependence should therefore remain linear, as is observed experimentally (Fig. 4). We can calculate the speed of sound $s \approx 1.5 \cdot 10^5$ cm/s and the mobility $\mu_0^{4,2} \approx s/E_{k_1}^0$ (equal to $3.75 \cdot 10^6$ cm²/V \cdot s for specimen Bi-3V16) from the relation $j_{k_1}^0 \approx nes$, where $n = n_{e2} + n_{e3} = 2 \cdot 10^{17}$ cm⁻³. This value of s agrees closely with the result in Ref. 28 for the fast shearing mode along the C_1 direction. We used the conductivities for $H = 0$ to calculate the electron mobilities in the other crystals (Table I).

The dependence of the acoustic emf E_a on the magnetic field strength H can be explained if longitudinal phonon generation occurs in the skin layer. Apparently, this dependence arises because the phonons increase in number in an angular interval $\theta \lesssim r/l_{ph} \ll \arccos(s/v_d)$ when a conducting channel of width $\sim r$ is present ($l_{ph} \approx 3 \cdot 10^{-2}$ according to Ref. 14). The relative number of radiated phonons (and hence also E_a) thus drops as H increases. The analogy here between "grazing" electrons and "grazing" phonons is quite plain—as $r/l_{ph} \rightarrow 0$, the latter give the dominant contribu-

tion to E_a . The increased frequency of collisions between energetic and thermal phonons¹⁴ is responsible for the temperature dependence $E_a(T)$ in Fig. 6.

2. Although no complete theory is yet available for the resistance of semimetal wires with circular cross section in a transverse magnetic field, we can use the formulas for the conductivity of plates to qualitatively explain the experimental results. According to Refs. 4 and 5, the average conductivity of a two-band isotropic semimetal is given by

$$\sigma_H^d \sim \sigma_H^\infty + \sigma_0^\infty (2L_1/d), \quad L_1 \ll r^2/l\tilde{d}, \quad (1)$$

$$\sigma_H^d \sim \sigma_H^\infty (1+l/\tilde{d}), \quad L_1 \gg r^2/l\tilde{d} \quad (2)$$

when a strong magnetic field parallel to the surface is present ($r \ll l, d$). Here σ_H^∞ and σ_0^∞ are the total conductivities of the electrons and holes in the limit $d \rightarrow \infty$; the current is concentrated in a diffusion layer of thickness L_1 . Since under our experimental conditions the electric current density was a maximum at distances $\sim r$ from the crystal surface, we can use the corresponding theoretical expression² to describe the results (it is easy to see³ that this expression must be modified by replacing \tilde{d} by q , where q is the diffusivity coefficient). In other words, we assume that $\tau_r \sim \tau$ in thin Bi single crystals of thickness $1-10 \mu\text{m}$, i.e., scattering by neutral impurities and defects is the dominant bulk relaxation mechanism.²⁹ Equation (2) coincides with the formula in Ref. 2 for the conductivity of a plate in a parallel magnetic field when $r/\tilde{d} \lesssim 1$, and it is convenient to rewrite it in the form

$$\sigma_H^d \sim \sigma_H^\infty + \sigma_0^\infty (r/l\tilde{d}) (2r/d), \quad (3)$$

where

$$\sigma_0^\infty (2r^2/l\tilde{d}) \sim (nec/H) (2r/\tilde{d}) \quad (4)$$

is the surface⁵⁾ conductivity σ_S .

2.1. The expressions for the average current density can be used to find the characteristic kink points on the I - V characteristic when longitudinal ($j_k \sim nes$) or transverse ($E_k \sim Hs/c$) phonon generation occurs. For $\tilde{d} \gg l/d$ ($\sigma_S \ll \sigma_H^\infty d$), the I - V characteristics are of the form¹⁰

$$\begin{aligned} j &\sim \sigma_H^\infty E, & E &\leq Hs/c, \\ j &\sim \sigma_H^\infty [E + (l/r)E_a], & E &\geq Hs/c. \end{aligned}$$

When $l/d \gg \tilde{d}$ (current concentrated in the skin layer),¹⁴

$$\begin{aligned} j &\sim \sigma_0^\infty (2r^2 E/\tilde{d}ld), & j &\leq nes(2r/d), \\ j &\sim \sigma_0^\infty (2r^2/\tilde{d}ld) (E - E_a), & j &\geq nes(2r/d), & E &\leq Hs/c. \end{aligned}$$

Figure 7 shows some schematic I - V characteristics in strong $E \times H$ fields; they contain several kink points which are due to supersonic carrier drifting. The changes in the derivative $\partial j/\partial E$ at the kinks are determined by the general principle that phonon generation along (transverse to) the current is associated with an increase (respectively, decrease) in the resistance.

When $\sigma_S \gg \sigma_H^\infty d$ the calculated field $E_{k_1}^H$ depends linearly on H , in qualitative agreement with experiment.⁶⁾ If we use the condition $E_{k_1}^H \sim sH\tilde{d}/c$ (Figs. 5, 7) to find the probability for intervalley scattering at the surface, we find that \tilde{d} differs considerably for specimens Bi-3V16 and Bi-10V2.

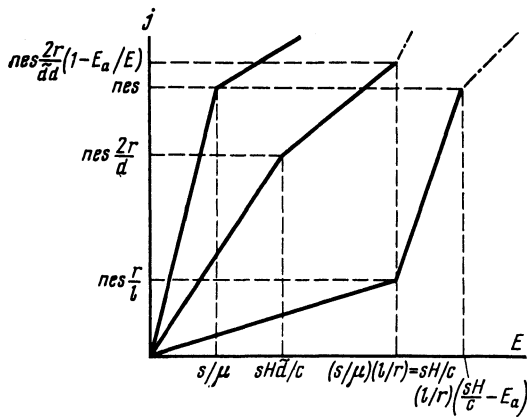


FIG. 7. Sketch showing I - V characteristics for a compensated semimetal in which longitudinal or transverse phonon generation occurs. The leftmost broken line corresponds to $H = 0$; for the middle line, $r \ll l$, $l/d \gg \tilde{d}$; for the rightmost line, $r \ll l$, $l/d \ll \tilde{d}$. The dashed-dotted extensions show portions of the I - V characteristics which were not observed experimentally.

This is very significant, because it indicates that relative changes in the probabilities for intervalley surface scattering of electrons and holes are responsible for the difference in the values of h found for these specimens.

We now consider the static skin effect for a two-band isotropic semimetal under the assumption that the hole contribution to the surface current is less than the electron contribution but is nonzero, i.e.,

$$j \sim \frac{nec}{Hd} \frac{2r_e}{\tilde{d}_e} \left(1 + \frac{r_p/\tilde{d}_p}{r_e/\tilde{d}_e} \right) E, \quad (5)$$

$$E_{k_1}^H \sim \frac{Hs}{c} \tilde{d}_e, \quad \frac{r_p/\tilde{d}_p}{r_e/\tilde{d}_e} = \alpha \ll 1.$$

It is clear that in this case the radius of the electron orbit must be found from the relation

$$j_{k_1}^H \sim nes 2r_e (1 + \alpha) / \tilde{d}, \quad (6)$$

where the coefficient $\alpha \propto \tilde{d}_e / \tilde{d}_p$ varies from specimen to specimen.

If we introduce an effective intervalley scattering probability $\tilde{d} \sim \tilde{d}_e / (1 + \alpha)$ and take $\alpha = 0$ for specimen Bi-10V2, we can use the formula

$$\rho_H^d \sim \sigma_n^{-1} d \sim \tilde{d} d (H/c)^2 / 2np_r \quad (7)$$

to calculate \tilde{d} for all the crystals which we investigated (Table I). The intervalley scattering probability at the surface generally increases with crystal thickness, as is also found from an analysis of the data in Ref. 6. Our values of \tilde{d} agree closely with the ones found there, and the methods used to prepare the crystals were also similar to some extent—most of the crystals in Ref. 6 were grown in quartz tubes, while we used Pyrex capillaries. By contrast, the probability for intervalley carrier scattering at the surface is much higher for specimens which are cut from massive ingots and then chemically polished.³⁰

In bulky bismuth crystals, the nonlinearity caused by longitudinal phonon generation in the skin layer⁷⁾ should be

observable at relatively low current densities. For example, current densities $j \lesssim 1$ A/cm² are typical for $d \gtrsim 10^{-1}$ cm, $H \sim 10$ kOe, and $\sigma_S \sim \sigma_H^{\infty} d$; for $l \lesssim 10^{-2}$ cm, these currents are less than 10% of the value required for transverse generation, and this should be borne in mind when analyzing nonlinearities in semimetals that contain bismuth. We note that no increase in the resistance preceding a positive jump in the slope at a kink point was reported in Refs. 9, 10, where the Esaki effect was analyzed. We may attribute this to the rather low surface conductivity of the specimens there, and to the large ($\sim 10\%$) experimental error due to the fact that the signals were recorded on an oscilloscope. Analysis of some results on the Esaki effect obtained by R. G. Valeev and one of the present authors reveals that the magnetoresistance is always 10–20% greater for $j \gtrsim 10$ A/cm², $E < Hs/c$ than for $j \sim 1$ A/cm² ($H \sim 5 \cdot 10^4$ Oe, $d \sim 10^{-1}$ cm, $T = 4.2$ K; $\sigma_H^{\infty} \gtrsim \sigma_S$). We note that the increase in the static magnetoresistance observed in Ref. 6 for bismuth in an electric field when $\sigma_S \gg \sigma_H^{\infty} d$ occurred precisely when $j \gtrsim 1$ A/cm². Setting $\tilde{d} \sim 10^{-2}$ (Ref. 6), we obtain $E_{k_1}^H \approx Hs\tilde{d}/c \sim 3 \cdot 10^{-2}$ V/cm for $H \approx 2.8$ kOe and $s \approx 10^5$ cm/s. This field is close to the corresponding value deduced from Fig. 10 in Ref. 6.

2.2 Gaïdukov and Golyamina in Ref. 18 also observed a temperature peak in the magnetoresistance for antimony whiskers, and like them, we attribute the peak to the static skin effect. However, our detailed interpretations differ somewhat; in Ref. 18 the experimental data were discussed using the theory in Ref. 2, which treats the linear term in the magnetoresistance. If we assume that $\sigma_S \gg \sigma_H^{\infty} d$ at low temperatures and take the surface intervalley scattering probability to increase with T , we find the condition

$$\frac{l}{\tilde{d}} (T_m) \sim d \quad (8)$$

for a maximum from relation (2).

According to (8), T_m is independent of H , in full agreement with experiment. However, if we use (1) to describe the experimental data, (8) is replaced by

$$l(T_m) \sim [dr(\tau_r/\tau)^{-1/2}]^{1/2}, \quad (9)$$

which implies that T_m depends on the magnetic field. For $\tau_r/\tau \sim 1$, (9) reduces to the corresponding condition in Ref. 18.

If we assume $\tilde{d} \sim 10^{-1}$ for the intervalley scattering probability for a Bi surface, and if we use³⁰

$$l \propto T^{-1} \text{ for } 30 < T < 70 \text{ K},$$

$$l \propto T^{-2} \text{ for } 4 < T < 30 \text{ K},$$

for specimens Bi-1A1 and Bi-3V18, which were of roughly identical quality, we find that $l(4.2 \text{ K}) \sim 10^{-2} - 10^{-3}$ cm. In a field $H \sim 10$ kOe, this corresponds to $r/l\tilde{d} \sim 10^{-1} - 1$, which demonstrates that Eqs. (2)–(4) correctly describe the experimental results. The dependence of T_m on the direction of the magnetic field vector observed for specimen Bi-10V1 may be ascribed to the anisotropy of the ratio (l/d) (T) for $T \lesssim 20$ K.

2.3 According to Ref. 31, the resistance of wires with $l \gg d$ is given in the absence of the magnetic field by

$$\rho_0^d \sim \rho_0^\infty + \rho_0^\infty (l/d) (1-P) (1+P)^{-1}, \quad (10)$$

where $P = 1 - q$ is the specularity coefficient. Setting $q \sim \tilde{d}$ as before and assuming $\rho_0^\infty \ll \rho_0^d, \sigma_H^d \ll \sigma_S$, we find using (10) and (3) that $r \sim d$ for the case when $\rho_0^d \sim \rho_H^d$ (Fig. 2), in qualitative agreement with experiment.

We close with the following observation. The temperature dependence of the diffusivity coefficient is usually attributed to electron scattering by surface phonons and to changes in the trajectory angle of the "grazing" electrons at the boundary of the crystal.³² According to the data in Ref. 33, the diffusivity coefficient for cadmium and zinc whiskers is almost equal to 1 even for $T \approx 20$ and 40 K. Under our conditions, only the temperature dependence of the electron scattering probability at the surface is important, although the extent to which this mechanism changes the specularity remains unclear.³² In any event, if we allow for a temperature-dependence $\tilde{d}(T)$, our results can be explained in the framework of a single closed model which yields electron mean-free paths l that are reasonable for highly pure bismuth. Heating could conceivably alter the surface charge distribution and widen the "cone of accessibility,"²⁹ thereby making intervalley scattering more likely. On the other hand, it could be that expressions (2)–(4) do not fully describe the physics of the static skin effect observed here (they then neglect the possible dependence of the surface conductivity σ_S on the mean free path l).

We are grateful to E. T. Lemeshevskaya for help with the experiment, and to A. I. Kopeliovich for some stimulating comments.

¹Extrapolation in the $\Delta R_H^d/H, H$ plane leads to unreliable results because the data do not lie on a straight line when plotted in terms of these coordinates, and the magnetoresistance was not measured systematically for $H < 1$ kOe.

²The pulsed measurements show that in the nonlinear regime, the relaxation times are of the same order of magnitude for finite and zero H (Ref. 14).

³The length $6.2 \cdot 10^{-5}$ cm corresponds to the experimental current $j_{k_1}^H$ at $H = 10.4$ kOe. Taking averages in the $j_{k_1}^H, H^{-1}$ plane (curve 1, Fig. 4), we find that $2h \approx 7.5 \cdot 10^{-5}$ cm.

⁴It also follows from Ref. 27 that $D_{\text{ext}}^e \approx 2.5 \cdot 10^{-5}$ cm, while $D_{\text{ext}}^p \approx 1.5 \cdot 10^{-5}$ cm.

⁵According to Ref. 2, the transverse magnetoconductivity of a slender wire ($l > d$) with $q = 1$ is $\sigma_H^d \sim \sigma_0^\infty (2r^2/d)$, which agrees with expression (3) when $\sigma_S \gg \sigma_H^d$ and $d = 1$.

⁶If we use Eq. (1) to describe the I - V characteristic for $\sigma_H^d \ll 2\sigma_0^\infty L_1$ (i.e., when the current is concentrated in the diffusion layer L_1), we find that $E_k \sim s/\mu_0$, which does not depend on the magnetic field.

⁷Except for cleavage planes, all surfaces are inevitably rough to some degree. According to Ref. 15, the current density is concentrated within a skin layer of thickness r if the magnetic field is inclined at an angle $\theta \gtrsim r/l$, ($l < d$) relative to the surface and $r/d \lesssim 1$.

¹M. Ya. Azbel', Zh. Eksp. Teor. Fiz. **44**, 983 (1963) [Sov. Phys. JETP **17**, 667 (1963)].

²V. G. Peschanskiĭ and M. Ya. Azbel', Zh. Eksp. Teor. Fiz. **55**, 1980 (1968) [Sov. Phys. JETP **28**, 1045 (1968)].

³A. I. Kopeliovich, Zh. Eksp. Teor. Fiz. **78**, 987 (1981) [Sov. Phys. JETP **51**, 498 (1981)].

⁴G. I. Babkin and V. Ya. Kravchenko, Zh. Eksp. Teor. Fiz. **60**, 695 (1971) [Sov. Phys. JETP **33**, 378 (1971)].

⁵A. I. Kopeliovich, Fiz. Nizk. Temp. **7**, 985 (1981) [Sov. J. Low Temp. Phys. **7**, 477 (1981)].

⁶S. S. Murzin, Zh. Eksp. Teor. Fiz. **82**, 515 (1982) [Sov. Phys. JETP **55**, 298 (1982)].

⁷V. F. Gantmakher and I. B. Levinson, Povekhnost'. Fiz., Khim., Mekh. **9**, 25 (1982).

⁸A. A. Lopez, Phys. Rev. **175**, 823 (1968).

⁹L. Esaki, Phys. Rev. Lett. **8**, 4 (1962).

¹⁰Yu. A. Bogod, Fiz. Nizk. Temp. **8**, 787 (1982) [Sov. J. Low Temp. Phys. **8**, 393 (1982)].

¹¹V. L. Gurevich, Fiz. Tekh. Poluprovodn. **2**, 1557 (1968) [Sov. Phys. Semicond. **2**, 1299 (1968)].

¹²V. I. Pustovoit, Usp. Fiz. Nauk **97**, 257 (1969) [Sov. Phys. Usp. **12**, 105 (1969)].

¹³Yu. A. Bogod, R. G. Valeev, D. V. Gitsu, and A. D. Grozav, Fiz. Nizk. Temp. **8**, 107 (1982) [Sov. J. Low Temp. **8**, 54 (1982)].

¹⁴Yu. A. Bogod, D. V. Gitsu, and A. D. Grozav, Zh. Eksp. Teor. Fiz. **84**, 2194 (1983) [Sov. Phys. JETP **57**, 1279 (1983)].

¹⁵D. V. Gitsu, A. D. Grozav, L. A. Konopko, and F. M. Muntyanu, Fiz. Tverd. Tela **25**, 2960 (1983) [Sov. Phys. Solid State **25**, 1707 (1983)].

¹⁶N. B. Brandt, D. V. Gitsu, A. M. Ioĭsher, B. P. Kotrubenko, and A. A. Nikolaeva, Prib. Tekh. Eksp., No. 3, 256 (1976).

¹⁷N. B. Brandt, D. V. Gitsu, A. A. Nikolaeva, and G. Ya. Ponomarev, Zh. Eksp. Teor. Fiz. **72**, 2332 (1977) [Sov. Phys. JETP **45**, 1226 (1977)].

¹⁸Yu. P. Gaĭdukov and E. M. Golyamina, Zh. Eksp. Teor. Fiz. **75**, 1465 (1978) [Sov. Phys. JETP **48**, 719 (1978)].

¹⁹Yu. A. Kirichenko and K. V. Rusanov, Teploobmen v Geliĭ-I v Uslovnykh Svobodnogo Dvizheniya (Heat Exchange in Free-Flowing Helium-I), Naukov Dumka, Kiev (1983).

²⁰B. P. Smolyakov and E. P. Khaĭmovich, Usp. Fiz. Nauk **136**, 317 (1982) [Sov. Phys. Usp. **25**, 102 (1982)].

²¹I. B. Levinson, Pis'ma Zh. Eksp. Teor. Fiz. **37**, 157 (1983) [JETP Lett. **37**, 190 (1983)].

²²Yu. V. Medvedev and V. F. Khirnyĭ, Fiz. Tverd. Tela **26**, 1163 (1984) [Sov. Phys. Solid State **26**, 705 (1984)].

²³B. A. Danil'chenko, V. V. Poroshin, and O. G. Sarbei, Pis'ma Zh. Eksp. Teor. Fiz. **38**, 386 (1983) [JETP Lett. **38**, 467 (1983)].

²⁴H. S. Carslaw and J. C. Jaeger, *Conduction of Heat in Solids*, 2nd ed., Clarendon Press, Oxford (1959).

²⁵L. Smith and N. M. Wolkott, Phil. Mag. **1**, 854 (1956).

²⁶G. K. White, *Experimental Techniques in Low-Temperature Physics*, Clarendon Press, Oxford (1959).

²⁷A. P. Korolyuk, Zh. Eksp. Teor. Fiz. **49**, 1009 (1965) [Sov. Phys. JETP **22**, 701 (1965)].

²⁸A. Eckstein, A. W. Lawson, and D. H. Reneker, J. Appl. Phys. **31**, 1534 (1960).

²⁹E. I. Rashba, Z. S. Gribnikov, and V. Ya. Kravchenko, in: *Elektrony Provodimosti (Conduction Electrons)*, M. I. Kaganov and V. S. Edel'man eds., Nauka, Moscow (1985), Chap. 9.

³⁰Yu. A. Bogod and V. B. Krasovitskiĭ, in: *Fizika Kondensirovannogo Sostoyaniya (Physics and the Condensed State)*, Khar'kov (1974), pp. 32, 38; Yu. A. Bogod, V. B. Krasovitskiĭ, and S. A. Mironov, Zh. Eksp. Teor. Fiz. **78**, 1099 (1980) [Sov. Phys. JETP **51**, 554 (1980)].

³¹R. B. Dingle, Proc. R. Soc. Ser. A **211**, 517 (1952).

³²Yu. P. Gaĭdukov, Usp. Fiz. Nauk **142**, 571 (1984) [Sov. Phys. Usp. **57**, 256 (1984)].

³³Yu. P. Gaĭdukov and Ya. Kadletsova, Zh. Eksp. Teor. Fiz. **59**, 700 (1970) [Sov. Phys. JETP **32**, 382 (1970)].

Translated by A. Mason